HHS Public Access

Author manuscript

Cancer Res. Author manuscript; available in PMC 2017 July 01.

Published in final edited form as:

Cancer Res. 2016 July 1; 76(13): 3978–3988. doi:10.1158/0008-5472.CAN-15-2834.

The tumor-associated glycosyltransferase ST6Gal-I regulates stem cell transcription factors and confers a cancer stem cell phenotype

Matthew J. Schultz[1], **Andrew T. Holdbrooks**[1], **Asmi Chakraborty**[1], **William E. Grizzle**[2], **Charles N. Landen**[3], **Donald J. Buchsbaum**[4], **Michael G. Conner**[5], **Rebecca C. Arend**[5], **Karina J Yoon**[6], **Christopher A. Klug**[7], **Daniel C. Bullard**[8], **Robert A. Kesterson**[8], **Patsy G. Oliver**[4], **Amber K. O'Connor**[1], **Bradley K. Yoder**[1], and **Susan L. Bellis**[1]

[1]Department of Cell, Developmental and Integrative Biology, University of Alabama at Birmingham (UAB), Birmingham, Alabama

[2]Department of Pathology, UAB, Birmingham, AL

[3]Department of Obstetrics and Gynecology, University of Virginia, Charlottesville, VA

[4]Department of Radiation Oncology, UAB, Birmingham, AL

[5]Department of Obstetrics and Gynecology, UAB, Birmingham, AL

[6]Department of Pharmacology, UAB, Birmingham, Alabama

[7]Department of Microbiology, UAB, Birmingham, Alabama

[8]Department of Genetics, UAB, Birmingham, Alabama

Abstract

The glycosyltransferase ST6Gal-I which adds α2-6-linked sialic acids to substrate glycoproteins has been implicated in carcinogenesis, however, the nature of its pathogenic role remains poorly understood. Here we show that ST6Gal-I is upregulated in ovarian and pancreatic carcinomas, enriched in metastatic tumors and associated with reduced patient survival. Notably, ST6Gal-I upregulation in cancer cells conferred hallmark cancer stem-like cell (CSC) characteristics. Modulating ST6Gal-I expression in pancreatic and ovarian cancer cells directly altered CSC spheroid growth, and clonal variants with high ST6Gal-I activity preferentially survived in CSC culture. Primary ovarian cancer cells from patient ascites or solid tumors sorted for α2-6 sialylation grew as spheroids, while cells lacking α2-6 sialylation remained as single cells and lost viability. ST6Gal-I also promoted resistance to gemcitabine and enabled the formation of stably-resistant colonies. Gemcitabine treatment of patient-derived xenograft tumors enriched for ST6Gal-I-expressing cells relative to pair-matched untreated tumors. ST6Gal-I also augmented tumor-initiating potential. In limiting dilution assays, subcutaneous tumor formation was inhibited by ST6Gal-I knockdown, whereas in a chemically-induced tumor initiation model, mice with conditional ST6Gal-I overexpression exhibited enhanced tumorigenesis. Lastly, we found that

Contact information: Susan L. Bellis, Ph.D., Department of Cell, Developmental and Integrative Biology, University of Alabama at Birmingham, MCLM982A 1918 University Blvd, Birmingham, AL 35294, bellis@uab.edu.

Conflict of interest: None of the authors have any conflicts to declare

ST6Gal-I induced expression of the key tumor-promoting transcription factors, Sox9 and Slug. Collectively this work highlighted a previously unrecognized role for a specific glycosyltransferase in driving a CSC state.

Introduction

Cancer Stem Cells (CSCs) are a subset of cancer cells endowed with the potential to initiate and recapitulate the original tumor. Intensive research is focused on the molecular identity of these cells, however studies of the CSC glycome are limited. One predominant glycan structure enriched in both cancer and stem cells is the α2–6 sialic acid linkage (1,2). The β-galactoside α2–6 sialyltransferase 1, ST6Gal-I, is the primary enzyme responsible for α2–6 sialylation of *N*-glycans on select glycoproteins (3), and its activity modulates cell adhesion, migration, differentiation, and survival (reviewed in (4,5)). As examples, ST6Gal-I-mediated α2–6 sialylation of the β1 integrin receptor promotes tumor cell migration and invasion (6–8), whereas α2–6 sialylation of the Fas and TNFR1 death receptors blocks apoptosis (9,10). EGFR is another ST6Gal-I substrate, and α2–6 sialylation of EGFR impedes cell death induced by the targeted therapeutic, gefitinib (11). ST6Gal-I activity also inhibits cell death induced by cisplatin (12), radiation (13) and galectins (14–16), highlighting the multiplicity of pathways through which ST6Gal-I serves as a tumor cell survival factor.

Increased ST6Gal-I mRNA in tumors is well-documented (reviewed in (17,18)), however few studies have evaluated ST6Gal-I protein in malignant or normal tissues. Previously we reported that ST6Gal-I protein was highly expressed in colon carcinomas, but largely absent from the normal differentiated colonic epithelium (19). Unexpectedly, a subset of ST6Gal-I-expressing cells was found within the base of colon crypts and basal epidermal layer, two known stem cell niches. As well, induced pluripotent stem (iPS) cells displayed a profound upregulation in ST6Gal-I relative to the fibroblasts from which they were derived (2,19–21), hinting that ST6Gal-I may have some stem cell-associated function. In colon cancer cells, ST6Gal-I expression correlates with two CSC markers, CD133 and Aldehyde Dehydrogenase 1 (ALDH1), and forced ST6Gal-I knockdown reduces the number of CD133/ALDH1-positive CSCs (19). In a microarray analysis, ST6Gal-I was one of the top 39 genes selectively expressed in CD133-positive, vs CD133-negative, colon CSCs (22).

In the current study we examined ST6Gal-I expression in ovarian and pancreatic cancer, and determined the role of ST6Gal-I in promoting CSC behaviors. ST6Gal-I levels were high in ovarian and pancreatic carcinomas, but negligible in the normal differentiated epithelium of these organs, suggesting that ST6Gal-I induction occurs during neoplastic transformation. ST6Gal-I activity confers archetypal CSC characteristics including spheroid growth, chemotherapy resistance, and tumor initiating potential. Strikingly, ST6Gal-I regulates the expression of two stem cell-associated transcription factors, Sox9 and Slug, known to play crucial roles in cancer initiation as well as maintenance of normal stem/progenitor pools. These findings elucidate a novel mechanistic pathway linking tumor cell glycosylation to the promotion of a CSC-like state.

Materials and Methods

Immunohistochemistry

Carcinoma tissues and patient ascites fluid were collected with informed consent and IRB approval. Paraffin-embedded tissues were incubated with anti-ST6Gal-I antibody (R&D systems, AF5924) (1μg/ml-5μg/ml) for 1 hour at room temperature using an IHC protocol extensively validated by our group (19). Developed slides were imaged with a Nikon Eclipse 80i camera and ISCapture software. Quantitative IHC scoring was conducted under blinded conditions by a pathologist. Survival curves for the ovarian adenocarcinoma cohort were evaluated by Logrank test.

Immunoblotting

Cells were lysed in RIPA buffer or 50 mM Tris buffer containing 1% Triton X supplemented with protease and phosphatase inhibitors (Sigma). Cancer tissues were homogenized by Polytron in Tris/Triton X-100 buffer and protein quantification was performed by BCA (Pierce). Immunoblots were probed with antibodies to ST6Gal-I (R&D systems, AF5924), Sox-9 (Santa Cruz, sc-0095, AbCam, ab26414, or Millipore, MABC672), Slug (Cell Signaling, 9585S), cleaved caspase 3 (Cell Signaling, 9654S), β-actin (AbCam), and β-tubulin (AbCam). Densitometry was performed with ImageJ software.

Cell Culture

BxPC3, MiaPaCa2, SKOV3, and HEK293 cells were purchased from ATCC. OV4 cells were obtained from Dr. Timothy Eberlein at Harvard University, Suit2 cells were from Dr. Michael A. Hollingsworth at the University of Nebraska, and HD3 cells were from Dr. Eileen Friedman at SUNY Syracuse. All lines were initially obtained several years ago, however upon receipt, the cells were immediately expanded to prepare frozen cell stocks. Cells have been tested to confirm lack of mycoplasma contamination, and some RNA Sequencing has been conducted, however, no additional authentication has been performed. Cells were grown in DME/F12 (OV4), RPMI (SKOV3, BxPC3, Suit2), or DMEM (MiaPaCa2, HEK293) containing 10% fetal bovine serum and antibiotic/antimycotic supplements (Invitrogen). HD3 cells were grown in low glucose DMEM with 7% FBS and antibiotics. Stable polyclonal lines expressing the human ST6Gal-I gene (Genecopoeia) or shRNA against ST6Gal-I (Sigma) were created by lentiviral transduction and puromycin selection. To verify that manipulation of ST6Gal-I expression resulted in altered ST6Gal-I activity, stably-transduced cells were stained with the SNA lectin (Vector), which binds α2–6 sialic acid, and then analyzed by flow cytometry (not shown). To monitor spheroid growth, cells were cultured in ultra-low adherence plates (Corning) in CSC media (DME/F12 or RPMI with 1x N1 supplement, 500μg/ml insulin, 20ng/ml EGF and 10ng/ml bFGF, Sigma). Spheroid growth was evaluated by ATP measurement (CellTiter-Glo, Promega). Primary cancer cells were isolated by centrifugation (ascites) or chemical and enzymatic dissociation (PDX tumors). Cells were stained with SNA-FITC (Vector) and sorted by FACS. SNA high and low populations were plated in CSC conditions, and spheroids counted from multiple fields.

Ascites Treatment

Fresh ovarian cancer ascites was centrifuged to remove cells. The remaining soluble fraction was mixed in varying amounts with serum-free media, and administered to OV4 cells. After 24 hours viability was assayed by a crystal violet assay. Three independent experiments were performed, with each experiment performed in triplicate.

Chemotherapy treatment

Unless otherwise indicated, gemcitabine (Selleck) treatments were performed at 100nM. Acute Gem treatment was evaluated by examining cleaved caspase 3 at 24hrs. Cell viability assays were conducted across a range of Gem dosages and time points using CellTiter-Glo (Promega). Three independent experiments were performed, with each experiment performed in triplicate. Treatment in spheroid conditions was performed for 5 days. Stable resistance was determined by continuous gemcitabine exposure for 10 days. Live/Dead cell viability staining (Invitrogen) was executed as the manufacturer recommends.

Patient-derived xenograft tumors

PDX models were maintained as in (23). Briefly, resected human pancreatic tumors were implanted into immunocompromised mice. When tumors reached ~200 mm^3, intraperitoneal injections of saline or Gem (200 mg/kg) were administered once a week for 6 weeks. Tumors were harvested, and embedded in paraffin blocks for analysis.

Limiting dilution tumor initiation assay

Animal procedures were done with prior approval from UAB IACUC. Cells were grown to 80–90% confluency, passaged, and resuspended in serum-free DMEM and kept on ice until injection. Cells were mixed 1:1 with Matrigel (Corning) and injected subcutaneously into the flanks of 5–6 week old, female, athymic nude mice (Harlan) at indicated dilutions (5 mice per group). Mice were evaluated 2–3 times per week for tumor formation and subsequent growth using digital calipers. Tumor volume was determined using the formula L x (W^2)/2.

Analysis of mPanINs

C57BL/6 mice with a conditionally active $Kras^{G12D}$ allele knocked into the endogenous *Kras* locus, or with the $Kras^{G12D}$ mutation combined with a conditionally activated, heterozygous deletion of tp53 ($Kras^{G12D}$;$tp53^{+/FL}$), were crossed with Pdx1-Cre mice to produce pancreas-specific expression or deletion of these factors. Mice were sacrificed at 3 months (Pdx1-Cre;$Kras^{G12D}$;$tp53^{+/FL}$) or 4 months (Pdx1-Cre;$Kras^{G12D}$), and pancreata were IHC-stained for ST6Gal-I.

Rosa26-ST6Gal-I mouse

C57BL/6 mice expressing ST6Gal-I under the Rosa-26 gene promoter were generated by the UAB Transgenic Mouse Facility. Briefly, the human ST6Gal-I CDS was amplified from a plasmid containing the *St6gal1* gene (Origene) and inserted into pRosa26-DEST (Addgene #21189).Primers used were:

Forward, BY3711:
ggggacaagtttgtacaaaaaagcaggcttaaccATGATTCACACCAACCTGAAG

Reverse, BY3712: ggggaccactttgtacaagaaagctgggtaTTAAACCTTATCGTCGTC

The ST6Gal-I targeting vector was electroporated into Primogenix B6 (C57BL/6 N-tac) embryonic stem (ES) cells. ES cells were injected into tyrosinase-deficient blastocysts to generate male chimeras. Germline passage was obtained by crossing chimeric males to albino C57BL/6 females.

Azoxymethane-Dextran Sulfate Sodium salt (AOM-DSS)

The Rosa26-ST6Gal-I mouse was crossed to a Villin-Cre mouse (The Jackson Laboratory, B6.Cg-Tg(Vil-cre)997Gum/J) to generate intestinal-specific ST6Gal-I overexpression on a C57BL/6 background. Eight Rosa-ST6^{+} Cre^{+} and eight Rosa-ST6^{+} Cre^{-} littermate control mice were evaluated by the AOM-DSS chemical carcinogenesis model as in (24). AOM was injected intraperitoneally (10 mg/kg body weight) and after one week, 2% DSS was added to the drinking water for 1 week. At 10 weeks, colons were evaluated for tumor formation. Tumor area was analyzed using ImageJ software.

ST6Gal-I Adenovirus

HEK293T cells were transduced with ST6Gal-I-expressing adenovirus (Applied Biological Materials) for 6 hours at MOIs of 100 and 1000. Cells were lysed after 48 hours and immunoblotted.

Results

ST6Gal-I is upregulated in ovarian carcinoma and correlates with decreased patient survival

Immunohistochemical (IHC) analyses of normal human ovary revealed minimal ST6Gal-I expression in epithelium and stroma (Fig.1A), although a subset of inclusion cysts expressed ST6Gal-I (not shown). In contrast, 34/35 ovarian serous adenocarcinomas (98%) were positive for ST6Gal-I. ST6Gal-I was present in tumor cells (Fig.1B, arrow), but not adjacent normal-appearing epithelium (arrowhead), and staining was heterogeneous, reflecting ST6Gal-I upregulation in specific tumor cell subpopulations. ST6Gal-I was also detected in immune cells within the tumor stroma (not shown), consistent with the known expression of ST6Gal-I in immune cells. Interestingly, we find a subset of ST6Gal-I-expressing cells within the normal fallopian tube (Fig.1C), a suggested stem cell reservoir and putative initiating site for ovarian cancer.

Accompanying survival data for patients in the ovarian serous adenocarcinoma cohort allowed a correlative analysis of ST6Gal-I IHC expression with progression-free survival (PFS) and overall survival (OS). Patients bearing tumors with high ST6Gal-I levels had significantly shortened survival by both measures (Fig.1D–E).

ST6Gal-I is upregulated in pancreatic cancer

We next evaluated a second organ, the normal and malignant pancreas, for ST6Gal-I expression by IHC. ST6Gal-I levels were minimal in normal acinar cells (Fig.1F, star), and most ductal cells (Fig.1F arrow), although a subset of the larger ducts was ST6Gal-I-positive (not shown). Some endocrine cells within the normal pancreatic islets expressed ST6Gal-I (Fig.1F, arrowhead), the function of which is unknown. In a cohort of epithelial pancreatic malignancies, including pancreatic ductal adenocarcinoma (PDAC), ST6Gal-I was expressed in 14/21 tumors (Fig.1G). ST6Gal-I was also observed in areas of chronic pancreatitis within tumors (not shown). Tissue was then obtained from 20 distinct pancreatic patient-derived xenograft (PDX) tumors. IHC revealed that 15/20 PDX tumors expressed ST6Gal-I (Fig. 1H). The primary pancreatic cancer cases, combined with PDX tumors, demonstrate 29/41 (71%) tumors positive for ST6Gal-I.

ST6Gal-I expression is enriched in metastatic tumors

To determine potential differences in ST6Gal-I expression as a result of metastasis, we examined 9 primary, and 10 metastatic, unmatched ovarian tumors. While ST6Gal-I was found in all tumor lysates by immunoblotting (Fig.2A, see long blot exposure; densitometry shown in Fig.2B), metastatic lysates showed a clear increase in ST6Gal-I (Fig.2C; densitometry shown in Fig.2D). Both full-length ST6Gal-I (∼50kD) and a ∼37kD known cleaved form (25) were detected. ST6Gal-I is cleaved by proteases including the BACE1 secretase (25). Consistent with other studies (19 and unpublished data), the cleaved ST6Gal-I isoform seems to be more abundant in tumor tissues compared with cultured cell lines, perhaps because of the proteolytic nature of the tumor microenvironment.

Sufficient tissue from the cohort described above was available for IHC analysis of all 9 primary, and 8/10 metastatic, tumors (representative images, Fig.2E–F). The average percentage of the tumor positive for ST6Gal-I was 60% in the primary cases, and 80% in the metastases (Fig.2G). The data was further segregated to group tumors that had 0–33%, 33–66%, or 66–100% ST6Gal-I-positive cells (Fig.2H). Primary tumors were distributed across the categories, whereas 7/8 metastatic tumors had > 66% ST6Gal-I-positive tumor cells. We also examined ST6Gal-I expression by IHC in 13 matched primary and metastatic ovarian tumors. Of these, 8 pairs had elevated ST6Gal-I expression in the metastases; 4 pairs had higher expression in the primary tumor, and 1 pair was unchanged. Together these results suggest that ST6Gal-I is elevated in the majority of metastatic cases.

ST6Gal-I contributes to spheroid growth

To interrogate the function of ST6Gal-I in CSC behavior, ST6Gal-I was stably knocked-down in the MiaPaCa2 and BxPC3 pancreatic cancer lines, and cells were evaluated for spheroid growth. Empty-vector control (EV) or ST6Gal-I-knockdown (ST6-KD) cells were grown for 2 weeks in CSC culture (nonadherent growth in serum-free media). As shown in Fig.3A–B, cell viability in spheroid conditions was decreased in ST6Gal-I knockdown cells. To confirm results in ovarian cancer cells, spheroid growth was monitored in the SKOV3 ovarian line. SKOV3 cells have relatively modest endogenous ST6Gal-I, therefore ST6Gal-I was both stably knocked-down (ST6-KD) and overexpressed (ST6-OE), in this line.

Viability in spheroid culture was diminished in ST6-KD cells, but enhanced in ST6-OE cells (Fig.3C).

Spheroid culture selects for ST6Gal-I-expressing clones

Spheroid culture is an established method for isolating CSCs; we thus hypothesized these conditions would select for subclones with high ST6Gal-I expression. SKOV3 cells were placed into standard, or CSC, culture for 1 week and ST6Gal-I expression was quantified in the surviving population. Higher ST6Gal-I levels were observed in EV cells grown in CSC conditions vs growth in FBS-containing media (Fig.3D). Significantly, ST6-OE and ST6-KD cells also exhibited enrichment in ST6Gal-I after placement in CSC culture (Fig.3D). These cell lines are pooled polyclonal populations, and both the shRNA and ST6Gal-I expression constructs are driven by constitutive promoters. Hence, increased ST6Gal-I levels in CSC spheroids likely result from selective survival of clones with high ST6Gal-I expression rather than transcriptional upregulation of the gene. Additionally, ST6Gal-I expression was examined at varying time points in MiaPaCa-2 and SKOV3 cells after placement in CSC culture, which revealed ST6Gal-I enrichment as a function of increasing time (Fig.3E–F).

Primary ovarian cancer cells sorted for ST6Gal-I activity selectively survive in spheroid culture

Tumor cell-rich ascites fluid was obtained from 3 ovarian cancer patients and the harvested cells were stained for ST6Gal-I. ST6Gal-I was expressed in the tumor spheroids of all 3 patients (representative image, Fig.3G). We then sorted fresh ascites cells by FACS using the SNA lectin which detects α2–6 sialic acids added by ST6Gal-I. SNA-high and SNA-low ascites cells were grown under CSC culture conditions. SNA-high cells formed spheroids, while SNA-low cells remained as single cells (Fig.3H–I). The SNA-high fraction survived in spheroid culture for at least a month, whereas the SNA-low population showed morphological signs of cell death after several days. This experiment was repeated with tumor cells dissociated from an ovarian cancer PDX tumor with similar results (Fig.3J).

ST6Gal-I promotes tumor cell survival within the ascites milieu

Ascites fluid represents a proinflammatory microenvironment which metastatic cells must navigate to seed tumors at distant sites. To test whether ST6Gal-I contributes to tumor cell survival within ascites, the cytokine-rich soluble fraction of ascites was collected (after removal of patient cells), and incubated with OV4 ovarian cancer cells which either lack ST6Gal-I (EV), or in which ST6Gal-I was stably expressed (ST6-OE). After 24 hours, EV cells exhibited marked cell death in the ascites microenvironment while ST6-OE cells were completely protected (Fig.3K). The graph depicts averages from 3 independent experiments using ascites from 3 distinct ovarian cancer patients, demonstrating that ST6Gal-I consistently protects against ascites-induced cell death despite potential patient-specific differences in ascites composition.

ST6Gal-I confers resistance to gemcitabine

Inherent chemoresistance is another known CSC characteristic; we therefore tested whether ST6Gal-I protects against gemcitabine (Gem), a frontline treatment for pancreatic cancer.

Compared with MiaPaCa2 EV cells, ST6-KD cells were sensitized to Gem-induced cell death, evidenced by increased caspase-3 cleavage (Fig.4A). We next examined the viability of cells exposed to Gem across a range of dosages and time points. At one day following Gem treatment, no major differences were noted in dose response (not shown). However, at 3 and 5 days after Gem treatment, KD cells exhibited significantly reduced survival compared with EV cells (Fig. 4B). Response to Gem was also examined in MiaPaCa2 spheroids, given that spheroids may better recapitulate the *in vivo* tumor response to chemotherapy than adherent cultures. As shown in Fig.4C, untreated EV cells exhibited more robust spheroid growth than untreated ST6-KD cells (consistent with results in Fig. 3A). However, significantly greater Gem-induced cell death was observed in ST6-KD cells after normalizing to the untreated controls; 57% cell death was measured for ST6-KD cells and 30% for EV cells ($p<0.05$). To assess ST6Gal-I involvement in stable Gem resistance, pancreatic cancer cells were exposed to prolonged, high-dose Gem (Fig.4D). For both BxPC3 and MiaPaCa2 lines, no apparent viable colonies were noted in the Gem-treated ST6-KD populations. Conversely, many viable colonies, measured by Live/Dead staining, were observed in the EV cultures.

ST6Gal-I expression is enriched in Gem-treated pancreatic patient-derived xenograft tumors

To evaluate ST6Gal-I's role in response to Gem treatment *in vivo*, pancreatic PDX tumors were harvested from mice treated with or without Gem, and immunostained for ST6Gal-I. We hypothesized that in heterogeneous tumor specimens, Gem treatment would enrich for ST6Gal-I-expressing cells due to a survival advantage conferred by ST6Gal-I. Tumors exposed to Gem *in vivo* had increased ST6Gal-I levels relative to pair-matched naïve tumors in 5/6 cases analyzed (representative pair in Fig.4E). In the single pair that did not show enrichment, ST6Gal-I was not detected in either control (saline) or Gem-treated tumors. These data, combined with *in vitro* studies of Gem-induced tumor cell death, suggest that ST6Gal-I contributes to a chemoresistant phenotype.

Tumor-initiating potential is enhanced by ST6Gal-I activity

To examine pancreatic tumor initiation, limiting dilution assays were conducted. EV or ST6-KD MiaPaCa2 cells were injected subcutaneously into immunocompromised mice at increasing dilutions and tumor incidence and growth were measured (Fig.5A–C). Tumors formed in all mice of both the EV and ST6-KD groups when 10^6 cells were injected. However, following injection with 10^5 cells, 5/5 mice in the EV group formed tumors compared with 3/5 mice in the ST6-KD group. ST6-KD-derived tumors were smaller in size, and tumors from the ST6-KD group took ~1 week longer to be detectable (Fig.5B). Additionally, two mice in the EV group, but none in the ST6-KD group, had lymph node metastases. At 10^4 cells injected, tumors formed in 3/5 mice in the EV group compared with 2/5 mice in the ST6-KD group (Fig.5C).

ST6Gal-I is upregulated in PanINs formed in genetically-engineered mouse models of pancreatic cancer

Consistent with a tumor-initiating function, it was anticipated that ST6Gal-I would be upregulated early in the neoplastic process. Human pancreatic cancer is thought to be

initiated by activating mutations in the *KRAS2* gene, present in >90% of advanced pancreatic cancers (26). To model this disease in mice, a mutated variant, $Kras^{G12D}$, is introduced in the pancreas by Cre-recombinase expressed under a pancreatic promoter *Pdx* (27). The *Pdx1-Cre;*$Kras^{G12D}$ mice develop preinvasive lesions (mPanIN) that closely resemble human preinvasive pancreatic intraepithelial lesions (PanIN), the precursor to PDAC. IHC analysis showed that ST6Gal-I was expressed in the mPanINs from *Pdx1-Cre;*$Kras^{G12D}$ mice (Fig.5D). Additionally, a second, more aggressive pancreatic cancer model with only a single copy of the tumor suppressor *tp53* in addition to $Kras^{G12D}$ (28) was examined. mPanINs from this second model also expressed ST6Gal-I (not shown). In both models, ST6Gal-I expression was noted in ductal-like cells undergoing acinar to ductal metaplasia (ADM) (not shown), a process thought to precipitate PanIN formation (29). In contrast, ST6Gal-I expression was only apparent in the islets of normal murine pancreata (Fig.5E).

Chemically-induced carcinogenesis is potentiated in ST6Gal-I transgenic mice

To further assess ST6Gal-I's role in cancer initiation, we utilized a well-established, chemically-induced colon carcinogenesis model in transgenic mice with intestinal-specific ST6Gal-I expression. ST6Gal-I with a floxed stop codon was engineered into the Rosa26 locus (Rosa-ST6Gal-I) and crossed to mice with Cre-recombinase expressed under the intestinal Villin promoter (Fig.5F). Azoxymethane-dextran sulfate sodium (AOM-DSS)-induced colon carcinogenesis (Fig.5G) was examined in 8 ST6Gal-I transgenic mice (Rosa-ST6Gal-I^+, Cre^+) and 8 control littermates (Rosa-ST6Gal-I^+, Cre^-). Mice expressing the ST6Gal-I transgene developed tumors in 8/8 cases while only 5/8 of the litter-matched controls formed tumors. The total area of tumor tissue (Fig.5H), as well as number of tumors per colon (Fig.5I), were significantly greater in ST6Gal-I transgenic mice.

ST6Gal-I regulates the expression of stem cell transcription factors Sox9 and Slug

Recent landmark studies suggest that *de novo* expression of the stem cell transcription factor, Sox9, in pancreatic acinar cells is the key initiating event in PDAC (29). Accordingly, MiaPaCa2 and BxPC3 pancreatic cells were immunoblotted for Sox9. As shown in Fig.6A–B, ST6Gal-I knockdown reduced the levels of Sox9. Similarly, Sox9 expression was repressed by ST6Gal-I knockdown in SKOV3 ovarian cancer cells, and HD3 colon cancer cells (Fig.6C–D). Contrarily, forced expression of ST6Gal-I in OV4 ovarian cancer cells induced Sox9 expression (Fig.6E). Suit2 pancreatic cancer cells were transduced with increasing amounts of lentivirus to produce populations with variant ST6Gal-I expression. In these lines, Sox9 protein increased in a dose dependent manner in correspondence with ST6Gal-I levels (Fig.6F). To evaluate ST6Gal-I regulation of Sox9 by an alternative method, HEK293 cells were transiently transduced with adenovirus to express ST6Gal-I. A marked increase in Sox9 was detected 48 hours after transduction (Fig.6G). Evidence suggests Sox9 acts in conjunction with the Slug (SNAI2) transcription factor to induce stemness (30), therefore we evaluated Slug expression in these lines. ST6Gal-I was found to regulate Slug in ovarian, but not pancreatic, cancer cells (Fig.6H–I). The finding that ST6Gal-I regulates expression of critical transcription factors such as Sox9 and Slug establishes a new role for cellular glycans in promoting stem-like cell properties.

Discussion

Aberrant surface glycosylation was one of the earliest-identified hallmarks of a tumor cell, however the functional role of specific glycosyltransferases in carcinogenesis remains unclear. Herein we show that ST6Gal-I is highly expressed in the majority of ovarian and pancreatic cancers, whereas levels are very low in the differentiated epithelium of these organs. Combined with similar observations in the colon (19), these results suggest ST6Gal-I upregulation is a common event in epithelial transformation (although notably, some specialized epithelia, such as the Brunner's glands and hepatocytes, express substantial ST6Gal-I, not shown). Supporting this concept, ST6Gal-I expression is induced in the early neoplastic lesions, mPanINs, that develop in two murine models of pancreatic carcinogenesis. In serous adenocarcinoma, the most prevalent and deadly subtype of ovarian cancer, ST6Gal-I expression correlates with decreased progression-free and overall patient survival, and is enriched in mestastases. Others have determined that tumor cell α2–6 sialylation promotes metastasis in animal models (31,32), and *in vitro* studies point to a role for ST6Gal-I in cell invasiveness (33–35). ST6Gal-I also facilitates epithelial-mesenchymal transition (EMT), an intermediate step in metastasis (36).

A prior, unanticipated finding was that ST6Gal-I expression in normal tissues is high in stem cell niches but not adjacent differentiated epithelia, suggesting that ST6Gal-I expression is repressed as cells transition away from the stem/progenitor compartment (19). Conversely, reversion of differentiated cells to a stem cell state by forced expression of pluripotency-inducing factors (Sox-2, Oct-4, Klf-4, and c-Myc) causes a dramatic induction of ST6Gal-I (2,19,20). In the polyoma middle T antigen breast cancer model, tumors arising in ST6Gal-I-null mice were more differentiated than those in wild type mice (37). Similarly, ST6Gal-I expression was inversely correlated with the level of differentiation in human colon tumors (38). The upstream mediators that control the dynamic expression of ST6Gal-I during cell differentiation or transformation are not well-defined, although oncogenic ras is known to stimulate ST6Gal-I expression (39,40). As well, ST6Gal-I expression is induced by the master stem cell transcription factor, Sox2 (41).

In view of the putative association between ST6Gal-I, stem/progenitor cells, and CSC markers (19), we hypothesized that ST6Gal-I is a molecular driver of CSC behaviors. Using cell models with forced ST6Gal-I overexpression or knockdown, we show ST6Gal-I regulates spheroid growth and response to gemcitabine. Moreover, cells with high endogenous ST6Gal-I exhibit a survival advantage when placed in spheroid culture, or after exposure to chemotherapy, both well-accepted methods for isolating CSCs from heterogeneous tumor cell populations. ST6Gal-I enrichment was also observed in pancreatic PDX tissues harvested from gemcitabine-treated, vs untreated, mice, providing *in vivo* evidence for the selective survival of cells with ST6Gal-I. The survival advantage conferred by ST6Gal-I extends to primary ovarian cancer cells isolated from solid tumors or patient ascites fluid. Ovarian cancer cells sorted for high levels of ST6Gal-I organized into spheroids and grew for a prolonged interval in CSC culture, while ST6Gal-I-deficient cells remained as single cells and did not survive initial seeding. We postulate ST6Gal-I may function to foster ovarian tumor cell survival within the peritoneal milieu, a critical event in ovarian cancer metastasis. To address this possibility, the acellular, cytokine-rich, soluble

fraction of patient ascites was incubated with ovarian cancer cell lines lacking endogenous ST6Gal-I or engineered with ST6Gal-I overexpression. Ascites-induced cell death was observed in cells devoid of ST6Gal-I, whereas ST6Gal-I-expressing cells were protected.

Our studies further suggest that ST6Gal-I participates in tumor initiation. In the AOM/DSS chemical carcinogenesis model, transgenic mice with forced ST6Gal-I expression had a greater number and overall area of colon tumors, relative to control littermates. As a second tumor initiation model, limiting dilution assays were conducted with pancreatic cancer cells with or without ST6Gal-I knockdown. At lower numbers of cells injected, fewer mice in the ST6Gal-I knockdown group developed tumors compared with controls, and the tumors that did form from knockdown cells were smaller in size. As well, some of the mice in the control group, but none in the ST6Gal-I knockdown group, developed lymph node metastases

Importantly, we find ST6Gal-I regulates the expression of a crucial tumor-initiating factor, Sox9, in pancreatic, ovarian and colon cancer cells. Sox9 is a stem cell-associated transcription factor strongly linked to the formation and growth of many types of cancer (42). In normal adult tissues, Sox9 is found in the basal colon crypt stem cell compartment (43), and is essential for maintaining the pool of pancreatic (44) and breast (45) progenitor cells. Sox9-dependent acinar to ductal reprogramming serves as the principal mechanism for initiation of PanINs and pancreatic ductal adenocarcinoma (29). Sox9 prevents cell senescence and cooperates with oncogenes such as ras to drive malignancy (46). Furthermore, Sox9 can act synergistically with the Slug transcription factor; Guo et al. reported that forced co-expression of Sox9 and Slug was sufficient to convert differentiated mammary cells into mammary stem cells (30). The finding that Sox9 and Slug expression are regulated by a specific glycosyltransferase implicates tumor glycosylation as a mechanism for functionally shifting cells to a less differentiated, stem-like state. In the aggregate, these studies highlight a novel function for the tumor glycome as an active contributor to the CSC phenotype.

Acknowledgments

Financial Support

This project was supported by NIH grants R01GM111093 and R21CA192629 (S.L. Bellis), the UAB/UMN SPORE in Pancreatic Cancer (P50CA101955, D.J. Buchsbaum), an NSF Graduate Research Fellowship (M.J. Schultz) and the UAB Howard Hughes Med to Grad Program (M.J. Schultz). Assistance was also received from the UAB Transgenic Mouse Core (NIH P30CA13148, P30AR048311, P30DK074038, P30DK05336, P60DK079626), Flow Cytometry Core (P30AR048311, P30AI027767), and Vector Production Facility.

References

1. Varki, A.; Kannagi, R.; Toole, BP. Glycosylation Changes in Cancer. In: Varki, A.; Cummings, RD.; Esko, JD., et al., editors. Essentials of Glycobiology. 2nd. Cold Spring Harbor (NY): Cold Spring Harbor Laboratory Press; 2009.
2. Hasehira K, Tateno H, Onuma Y, Ito Y, Asashima M, Hirabayashi J. Structural and quantitative evidence for dynamic glycome shift on production of induced pluripotent stem cells. Mol Cell Proteomics. 2012; 11:1913–1923. [PubMed: 23023295]

3. Martin LT, Marth JD, Varki A, Varki NM. Genetically altered mice with different sialyltransferase deficiencies show tissue-specific alterations in sialylation and sialic acid 9-O-acetylation. J Biol Chem. 2002; 277:32930–32938. [PubMed: 12068010]
4. Schultz MJ, Swindall AF, Bellis SL. Regulation of the metastatic cell phenotype by sialylated glycans. Cancer Metastasis Rev. 2012; 31:501–518. [PubMed: 22699311]
5. Lu J, Gu J. Significance of beta-galactoside alpha2,6 sialyltranferase 1 in cancers. Molecules. 2015; 20:7509–7527. [PubMed: 25919275]
6. Seales EC, Jurado GA, Brunson BA, Wakefield JK, Frost AR, Bellis SL. Hypersialylation of beta1 integrins, observed in colon adenocarcinoma, may contribute to cancer progression by up-regulating cell motility. Cancer Res. 2005; 65:4645–4652. [PubMed: 15930282]
7. Shaikh FM, Seales EC, Clem WC, Hennessy KM, Zhuo Y, Bellis SL. Tumor cell migration and invasion are regulated by expression of variant integrin glycoforms. Exp Cell Res. 2008; 314:2941–2950. [PubMed: 18703050]
8. Lee M, Park JJ, Ko YG, Lee YS. Cleavage of ST6Gal I by radiation-induced BACE1 inhibits golgi-anchored ST6Gal I-mediated sialylation of integrin beta1 and migration in colon cancer cells. Radiat Oncol. 2012; 7:47. [PubMed: 22449099]
9. Swindall AF, Bellis SL. Sialylation of the Fas death receptor by ST6Gal-I provides protection against Fas-mediated apoptosis in colon carcinoma cells. J Biol Chem. 2011; 286:22982–22990. [PubMed: 21550977]
10. Liu Z, Swindall AF, Kesterson RA, Schoeb TR, Bullard DC, Bellis SL. ST6Gal-I regulates macrophage apoptosis via alpha2-6 sialylation of the TNFR1 death receptor. J Biol Chem. 2011; 286:39654–39662. [PubMed: 21930713]
11. Park JJ, Yi JY, Jin YB, Lee YJ, Lee JS, Lee YS, et al. Sialylation of epidermal growth factor receptor regulates receptor activity and chemosensitivity to gefitinib in colon cancer cells. Biochem Pharmacol. 2012; 83:849–857. [PubMed: 22266356]
12. Schultz MJ, Swindall AF, Wright JW, Sztul ES, Landen CN, Bellis SL. ST6Gal-I sialyltransferase confers cisplatin resistance in ovarian tumor cells. J Ovarian Res. 2013; 6:25. [PubMed: 23578204]
13. Lee M, Park JJ, Lee YS. Adhesion of ST6Gal I-mediated human colon cancer cells to fibronectin contributes to cell survival by integrin beta1-mediated paxillin and AKT activation. Oncol Rep. 2010; 23:757–761. [PubMed: 20127017]
14. Zhuo Y, Bellis SL. Emerging role of alpha2,6-sialic acid as a negative regulator of galectin binding and function. J Biol Chem. 2011; 286:5935–5941. [PubMed: 21173156]
15. Toscano MA, Bianco GA, Ilarregui JM, Croci DO, Correale J, Hernandez JD, et al. Differential glycosylation of TH1, TH2 and TH-17 effector cells selectively regulates susceptibility to cell death. Nat Immunol. 2007; 8:825–834. [PubMed: 17589510]
16. Amano M, Galvan M, He J, Baum LG. The ST6Gal I sialyltransferase selectively modifies N-glycans on CD45 to negatively regulate galectin-1-induced CD45 clustering, phosphatase modulation, and T cell death. J Biol Chem. 2003; 278:7469–7475. [PubMed: 12499376]
17. Dall'Olio F, Chiricolo M. Sialyltransferases in cancer. Glycoconjugate J. 2001; 18:841–850.
18. Dall'Olio F, Malagolini N, Trinchera M, Chiricolo M. Sialosignaling: Sialyltransferases as engines of self-fueling loups in cancer-progression. Biochim Biophys Acta. 2014; 1840:2752–2764. [PubMed: 24949982]
19. Swindall AF, Londono-Joshi AI, Schultz MJ, Fineberg N, Buchsbaum DJ, Bellis SL. ST6Gal-I protein expression is upregulated in human epithelial tumors and correlates with stem cell markers in normal tissues and colon cancer cell lines. Cancer Res. 2013; 73:2368–2378. [PubMed: 23358684]
20. Tateno H, Toyota M, Saito S, Onuma Y, Ito Y, Hiemori K, et al. Glycome diagnosis of human induced pluripotent stem cells using lectin microarray. J Biol Chem. 2011; 286:20345–20353. [PubMed: 21471226]
21. Wang YC, Stein JW, Lynch CL, Tran HT, Lee CY, Coleman R, et al. Glycosyltransferase ST6GAL1 contributes to the regulation of pluripotency in human pluripotent stem cells. Sci Rep. 2015; 5:13317. [PubMed: 26304831]

22. Ieta K, Tanaka F, Haraguchi N, Kita Y, Sakashita H, Mimori K, et al. Biological and genetic characteristics of tumor-initiating cells in colon cancer. Ann Surg Oncol. 2008; 15:638–648. [PubMed: 17932721]

23. Garcia PL, Council LN, Christein JD, Arnoletti JP, Heslin MJ, Gamblin TL, et al. Development and histopathological characterization of tumorgraft models of pancreatic ductal adenocarcinoma. PLoS One. 2013; 8:e78183. [PubMed: 24194913]

24. Tanaka T, Kohno H, Suzuki R, Yamada Y, Sugie S, Mori H. A novel inflammation-related mouse colon carcinogenesis model induced by azoxymethane and dextran sodium sulfate. Cancer Sci. 2003; 94:965–973. [PubMed: 14611673]

25. Kitazume S, Tachida Y, Oka R, Shirotani K, Saido TC, Hashimoto Y. Alzheimer's beta-secretase, beta-site amyloid precursor protein-cleaving enzyme, is responsible for cleavage secretion of a Golgi-resident sialyltransferase. Proc Natl Acad Sci. 2001; 98:13554–13559. [PubMed: 11698669]

26. Almoguera C, Shibata D, Forrester K, Martin J, Arnheim N, Perucho M. Most human carcinomas of the exocrine pancreas contain mutant c-K-ras genes. Cell. 1988; 53:549–554. [PubMed: 2453289]

27. Hingorani SR, Petricoin EF, Maitra A, Rajapakse V, King C, Jacobetz MA, et al. Preinvasive and invasive ductal pancreatic cancer and its early detection in the mouse. Cancer Cell. 2003; 4:437–450. [PubMed: 14706336]

28. Hingorani SR, Wang L, Multani AS, Combs C, Deramaudt TB, Hruban RH, et al. Trp53R172H and KrasG12D cooperate to promote chromosomal instability and widely metastatic pancreatic ductal adenocarcinoma in mice. Cancer Cell. 2005; 7:469–483. [PubMed: 15894267]

29. Kopp JL, von Figura G, Mayes E, Liu FF, Dubois CL, Morris JP4th, et al. Identification of Sox9-dependent acinar-to-ductal reprogramming as the principal mechanism for initiation of pancreatic ductal adenocarcinoma. Cancer Cell. 2012; 22:737–750. [PubMed: 23201164]

30. Guo W, Keckesova Z, Donaher JL, Shibue T, Tischler V, Reinhardt F, et al. Slug and Sox9 cooperatively determine the mammary stem cell state. Cell. 2012; 148:1015–1028. [PubMed: 22385965]

31. Bresalier RS, Rockwell RW, Dahiya R, Duh QY, Kim YS. Cell surface sialoprotein alterations in metastatic murine colon cancer cell lines selected in an animal model for colon cancer metastasis. Cancer Res. 1990; 50:1299–1307. [PubMed: 2297775]

32. Harvey BE, Toth CA, Wagner HE, Steele GD Jr, Thomas P. Sialyltransferase activity and hepatic tumor growth in a nude mouse model of colorectal cancer metastases. Cancer Res. 1992; 52:1775–1779. [PubMed: 1312899]

33. Christie DR, Shaikh FM, Lucas JA4th, Lucas JA 3rd, Bellis SL. ST6Gal-I expression in ovarian cancer cells promotes an invasive phenotype by altering integrin glycosylation and function. J Ovarian Res. 2008; 1:3. [PubMed: 19014651]

34. Lin S, Kemmner W, Grigull S, Schlag PM. Cell surface alpha 2,6 sialylation affects adhesion of breast carcinoma cells. Exp Cell Res. 2002; 276:101–110. [PubMed: 11978012]

35. Zhu Y, Srivatana U, Ullah A, Gagneja H, Berenson CS, Lance P. Suppression of a sialyltransferase by antisense DNA reduces invasiveness of human colon cancer cells in vitro. Biochim Biophys Acta. 2001; 1536:148–160. [PubMed: 11406350]

36. Lu J, Isaji T, Im S, Fukuda T, Hashii N, Takakura D, et al. beta-galactoside alpha2,6-sialyltranferase 1 promotes transforming growth factor-beta-mediated epithelial-mesenchymal transition. J Biol Chem. 2014; 289:34627–34641. [PubMed: 25344606]

37. Hedlund M, Ng E, Varki A, Varki NM. alpha 2-6-Linked sialic acids on N-glycans modulate carcinoma differentiation in vivo. Cancer Res. 2008; 68:388–394. [PubMed: 18199532]

38. Gangopadhyay A, Perera SP, Thomas P. Differential expression of alpha2,6-sialyltransferase in colon tumors recognized by a monoclonal antibody. Hybridoma. 1998; 17:117–123. [PubMed: 9627051]

39. Seales EC, Jurado GA, Singhal A, Bellis SL. Ras oncogene directs expression of a differentially sialylated, functionally altered beta1 integrin. Oncogene. 2003; 22:7137–7145. [PubMed: 14562042]

40. Dalziel M, Dall'Olio F, Mungul A, Piller V, Piller F. Ras oncogene induces beta-galactoside alpha2,6-sialyltransferase (ST6Gal I) via a RalGEF-mediated signal to its housekeeping promoter. Eur J Biochem. 2004; 271:3623–3634. [PubMed: 15355339]

41. Boumahdi S, Driessens G, Lapouge G, Rorive S, Nassar D, Le Mercier M, et al. SOX2 controls tumour initiation and cancer stem-cell functions in squamous-cell carcinoma. Nature. 2014; 511:246–250. [PubMed: 24909994]

42. Jo A, Denduluri S, Zhang B, Wang Z, Yin L, Yan Z, et al. The versatile functions of Sox9 in development, stem cells, and human diseases. Genes Dis. 2014; 1:149–161. [PubMed: 25685828]

43. Blache P, van de Wetering M, Duluc I, Domon C, Berta P, Freund JN, et al. SOX9 is an intestine crypt transcription factor, is regulated by the Wnt pathway, and represses the CDX2 and MUC2 genes. J Cell Biol. 2004; 166:37–47. [PubMed: 15240568]

44. Seymour PA, Freude KK, Tran MN, Mayes EE, Jensen J, Kist R, et al. SOX9 is required for maintenance of the pancreatic progenitor cell pool. Proc Natl Acad Sci. 2007; 104:1865–1870. [PubMed: 17267606]

45. Malhotra GK, Zhao X, Edwards E, Kopp JL, Naramura M, Sander M, et al. The role of Sox9 in mouse mammary gland development and maintenance of mammary stem and luminal progenitor cells. BMC Dev Biol. 2014; 14:47. [PubMed: 25527186]

46. Matheu A, Collado M, Wise C, Manterola L, Cekaite L, Tye AJ, et al. Oncogenicity of the developmental transcription factor Sox9. Cancer Res. 2012; 72:1301–1315. [PubMed: 22246670]

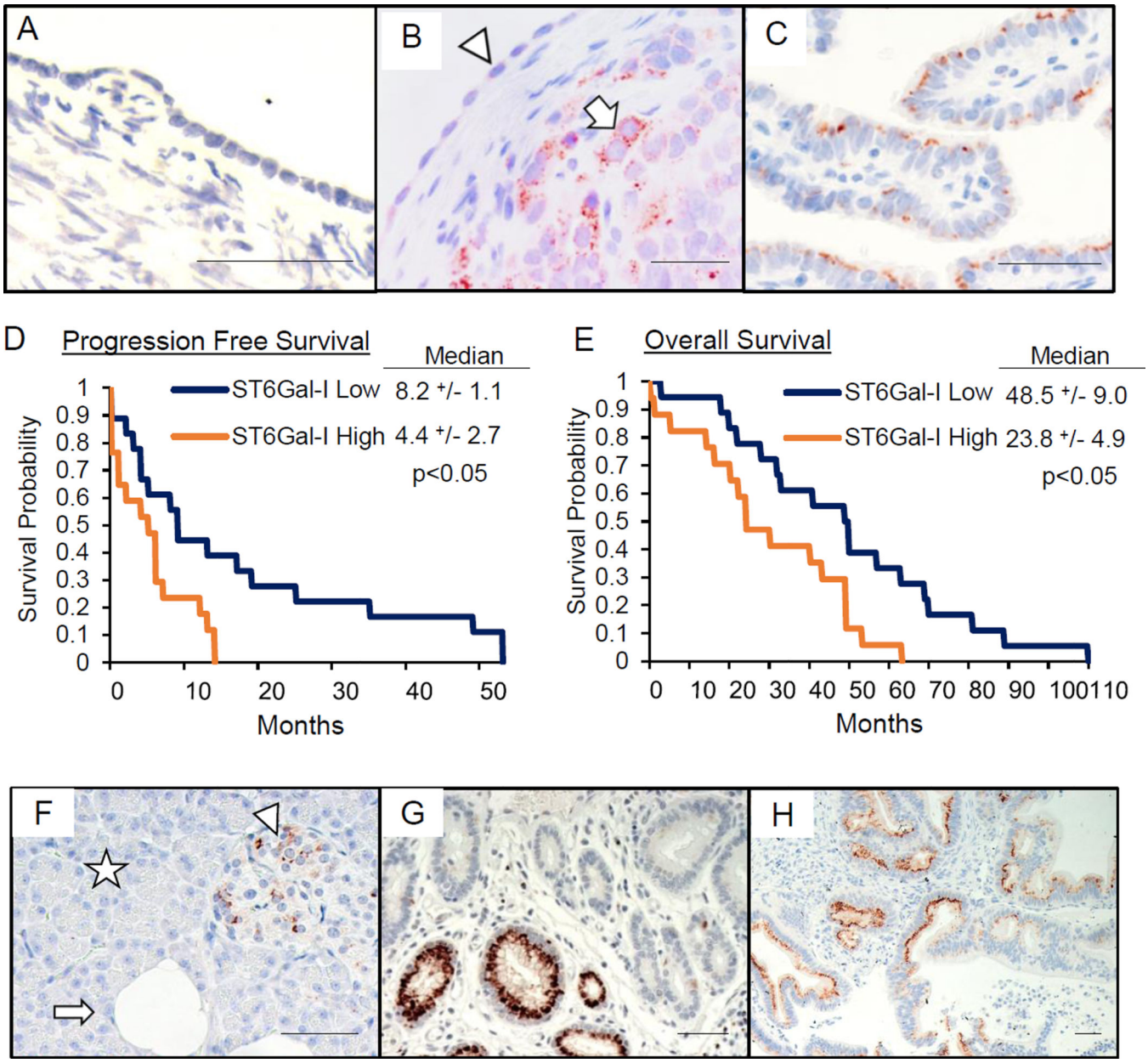

Fig. 1. ST6Gal-I is upregulated in ovarian and pancreatic carcinoma and correlates with patient survival

(A–C) ST6Gal-I expression by IHC in: (A) normal ovarian epithelium and stroma; (B) ovarian tumor with ST6Gal-I-positive tumor cells (arrow), adjacent to ST6Gal-I-negative, normal-appearing epithelium (arrowhead); and (C) normal fallopian tube epithelium. Scale bars=50μm. ST6Gal-I expression correlated with (D) progression free and (E) overall survival. (F–H) IHC for ST6Gal-I in: (F) normal pancreas with acinar (star) and ductal (arrow) cells, and pancreatic islets (arrowhead); (G) pancreatic adenocarcinoma; (H) pancreatic PDX tumor. Scale bars=50μm.

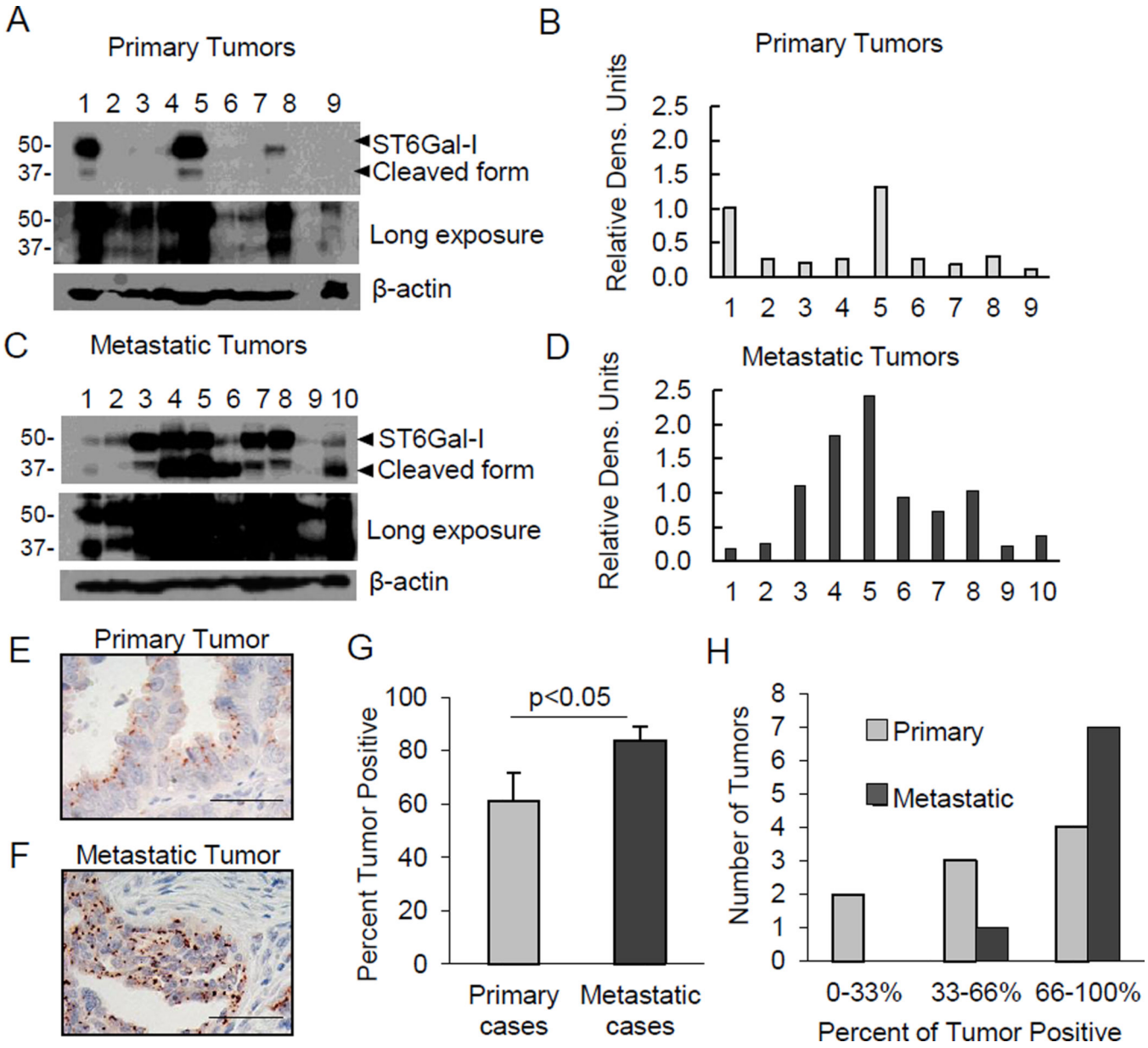

Fig. 2. ST6Gal-I is enriched in metastatic tumors

(A–B) Immunoblot and densitometry (normalized to β-actin) for ST6Gal-I in primary ovarian tumors. (C–D) Immunoblot and densitometry for unmatched metastatic tumors. (E–F) IHC images of a primary and metastatic tumor stained for ST6Gal-I. Scale bars=50μm. (G) Percentage of ST6Gal-I-positive cells within primary and metastatic tumors. Values = means and S.E.; *denotes $p<0.05$, Student's t-test. (H) Tumors grouped into low, middle, or high percentage of ST6Gal-I-positive cells.

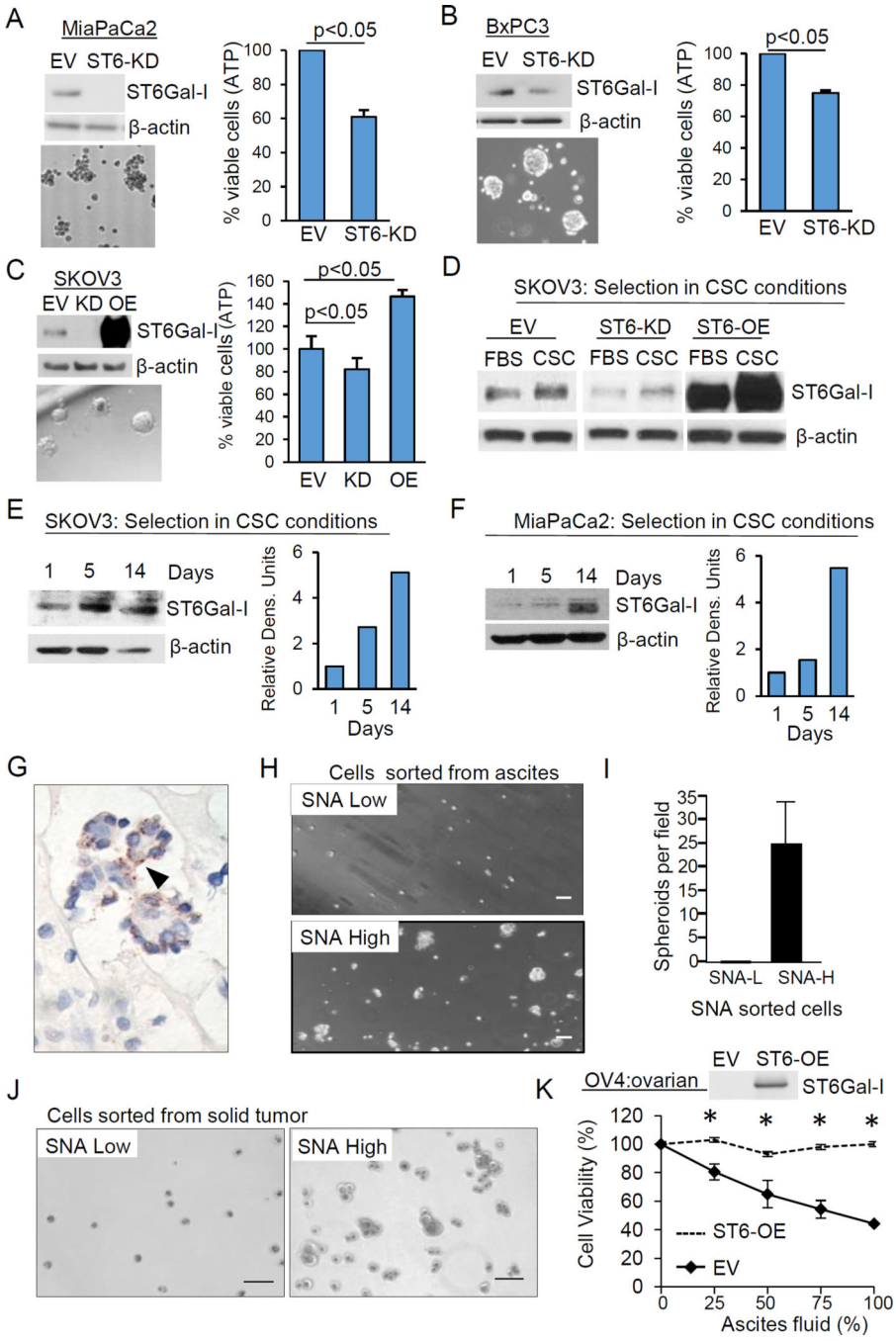

Fig. 3. ST6Gal-I promotes survival of CSC spheroids

(A–B) Viability of MiaPaCa2 (A) and BxPC3 (B) empty vector (EV) and ST6Gal-I knockdown (ST6-KD) cells grown in CSC culture for two weeks. (C) Viability of SKOV3 EV, ST6-KD or ST6Gal-I overexpressing (ST6-OE) cells in CSC culture. Values = means and S.E. for 3 independent experiments, $p<0.05$; Student's t test. (D) Immunoblot of SKOV3 cells cultured in CSC vs standard 10% FBS-containing media for 1 week. (E–F) ST6Gal-I immunoblotting and densitometry for SKOV3 (E) or MiaPaCa2 (F) cells cultured in CSC media for 1, 5, or 14 days. (G) ST6Gal-I expression (arrowhead) in ovarian ascites

tumorspheroid. (H) SNA high (SNA-H) and SNA low (SNA-L) ascites cells grown in CSC culture. (I) Spheroids per field. (J) Ovarian PDX tumor SNA-H and SNA-L grown in CSC culture. (K) Viability of OV4 EV or ST6-OE cells incubated in cell-free ascites. Values = means and S.E., $p<0.05$; Student's t-test. Scale bars=50μm.

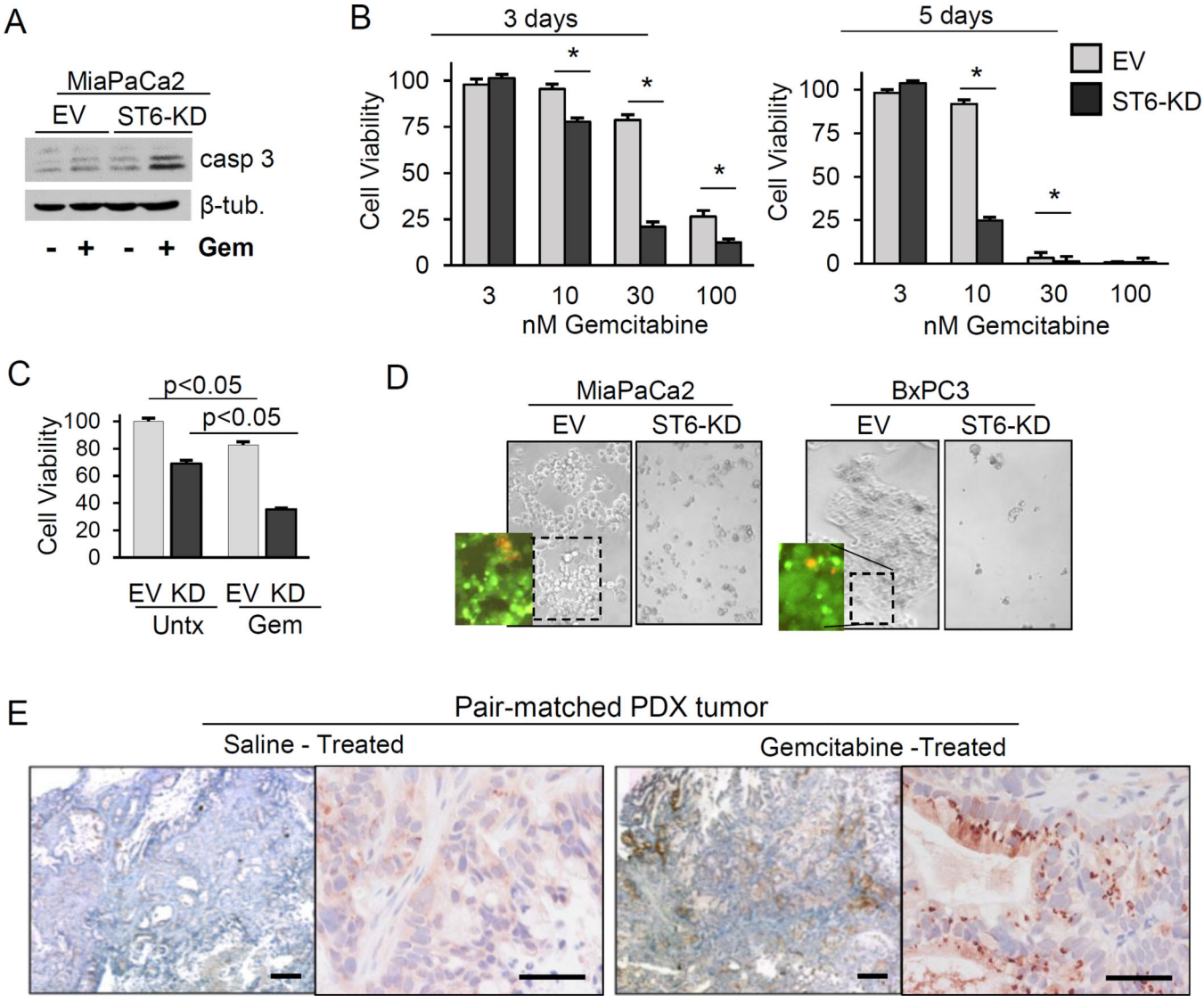

Fig. 4. ST6Gal-I confers gemcitabine resistance

(A) MiaPaCa2 EV and ST6-KD cells were immunoblotted for cleaved caspase-3 after a 24-hr treatment with 100nM Gem. (B) CellTiter-Glo assays were conducted to assess the viability of MiaPaCa2 EV and ST6-KD cells treated with Gem for 3 or 5 days. * = $p<0.05$ by student's t-test. (C) Viability of CSC spheroids treated with 100 nM Gem for 5 days. (D) Adherent MiaPaCa2 and BxPC3 cells exposed to 100 nM Gem for 10 days. Insets show live (green) and dead (red) cells. (E) ST6Gal-I expression in pair-matched, pancreatic PDX tumors from saline- or Gem-treated mice. Scale bars = 500μm (left panel, each pair) and 50 μm (right panel, each pair).

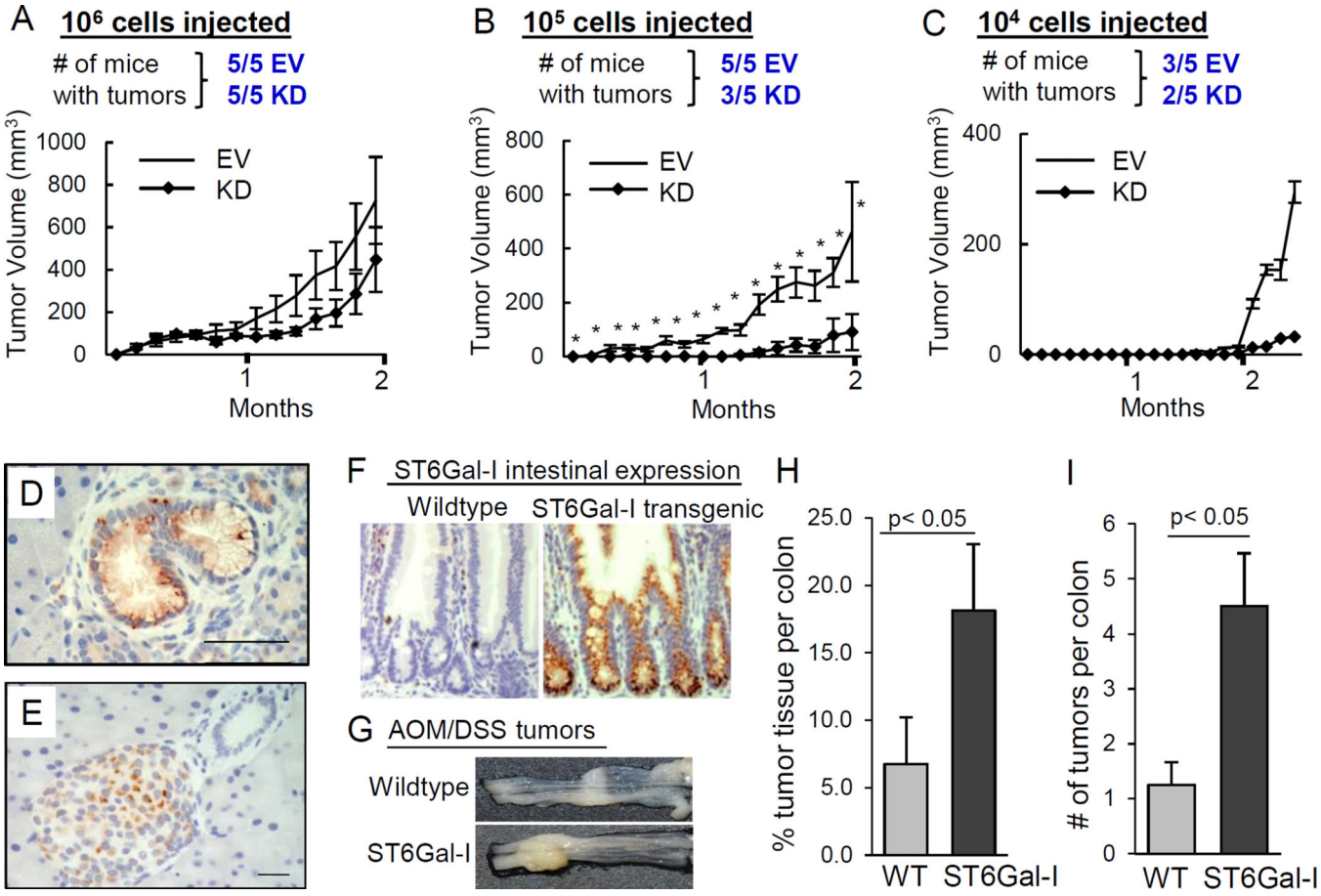

Fig. 5. ST6Gal-I contributes to tumor initiation

(A–C) Tumor incidence and growth for mice injected with 10^6 (A), 10^5 (B), or 10^4 (C) cells. *p<0.05. (D–E) ST6Gal-I expression in: (D) mPanINs from $Kras^{G12D}$ mice; (E) normal murine pancreas. Scale bars=50μm. (F) ST6Gal-I expression in intestines of Rosa-ST6Gal-I^+/Cre^- mice (wildtype) or ST6Gal-I^+/Cre^+ transgenic mice (ST6Gal-I knock-in). (G) Representative colon tissues following AOM-DSS treatment. (H) Percent area of tumor tissue per colon in wildtype (WT) or ST6Gal-I knock-in (ST6Gal-I) mice. (I) Tumor number per colon. Values = means and S.E.; p<0.05, Student's t-test.

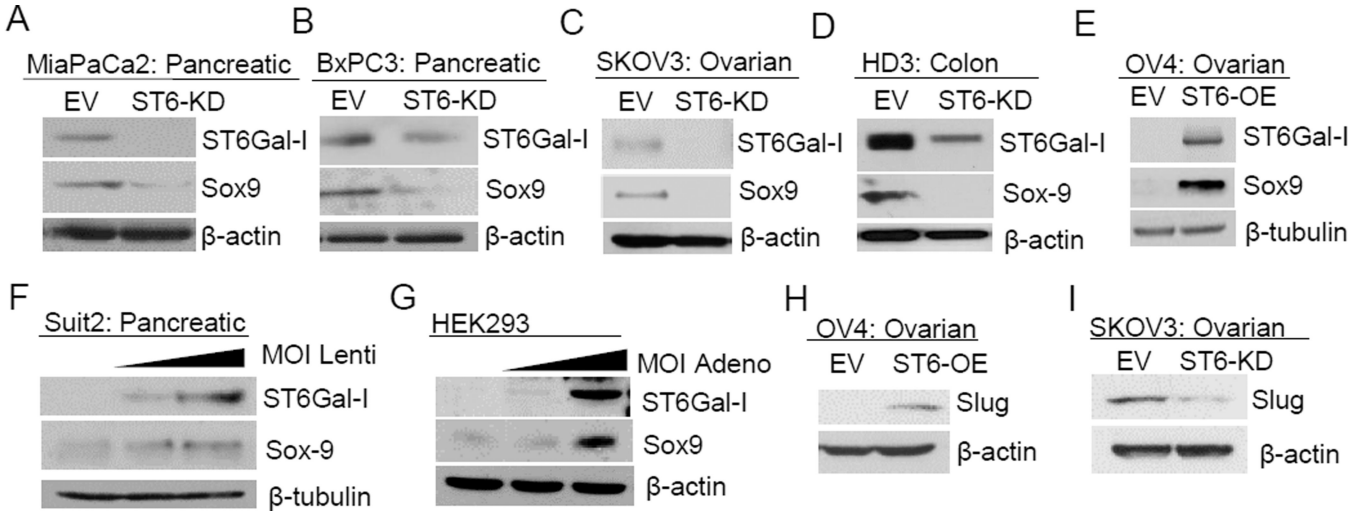

Fig. 6. ST6Gal-I regulates Sox9 and Slug expression

(A–D) Sox9 expression is repressed by ST6Gal-I knockdown. (E) Sox9 is induced by forced ST6Gal-I expression. (F) Suit2 cancer cells transduced with increasing amounts of ST6Gal-I lentivirus exhibit a dose-dependent Sox9 increase. (G) Sox9 is induced in HEK293 transduced with ST6Gal-I-expressing adenovirus. (H) Slug expression is induced in OV4 ST6-OE cells, but (I) decreased in SKOV3 ST6-KD cells.